Applied Catalysis B: Environmental 239 (2018) 654–664

Contents lists available at ScienceDirect

Applied Catalysis B: Environmental

journal homepage: www.elsevier.com/locate/apcatb

Aqueous-phase hydrodechlorination of trichloroethylene over Pd-based swellable organically-modified silica (SOMS): Catalyst deactivation due to chloride anions

Gokhan Celik[a], Saurabh A. Ailawar[a], Seval Gunduz[a], Jeffrey T. Miller[b], Paul L. Edmiston[c], Umit S. Ozkan[a,*]

[a] William G. Lowrie Department of Chemical and Biomolecular Engineering, The Ohio State University, 151 W. Woodruff Avenue, Columbus, OH, 43210, USA
[b] Davidson School of Chemical Engineering, Purdue University, 480 Stadium Mall Drive, West Lafayette, IN, 47907-2100, USA
[c] Department of Chemistry, The College of Wooster, 943 College Mall, Wooster, OH, 44691, USA

ARTICLE INFO

Keywords:
Swellable organically-modified silica (SOMS)
Palladium
Swelling
Pd/Al_2O_3
Hydrodechlorination
Deactivation
Hydrophobicity

ABSTRACT

Swellable-organically modified silica (SOMS) has been demonstrated to be an efficient catalyst scaffold for catalytic treatment of water contaminated with trichloroethylene (TCE). In this study, deactivation characteristics of Pd-incorporated SOMS for aqueous-phase hydrodechlorination (HDC) of TCE were investigated. Pd/SOMS catalysts were exposed to highly-concentrated chloride solutions (up to 1 M NaCl or 0.01 M HCl) to examine the deactivation resistant behavior of Pd/SOMS. The commonly used HDC catalyst Pd/Al_2O_3 was also studied for comparison purposes. Pd/SOMS and Pd/Al_2O_3 in their pristine and treated states were tested for aqueous-phase HDC of TCE and characterized by several techniques including N_2 physisorption, inductively coupled plasma optical emission spectroscopy (ICP-OES), X-ray photoelectron spectroscopy, extended X-ray absorption fine structure spectroscopy (EXAFS), and diffuse reflectance infrared Fourier transform spectroscopy (DRIFTS) of adsorbed CO. The aqueous-phase treatments had a pronounced adverse effect on the textural properties of Pd/Al_2O_3, although the effect was independent of the type of the chloride precursor, NaCl or HCl. Treating Pd/Al_2O_3 with chloride-containing solutions lowered the catalytic activity due to formation of Pd-Cl complexes and active metal leaching. The leached Pd obtained from the treatment solution was shown to be inactive for aqueous-phase HDC of TCE. While Pd/Al_2O_3 underwent severe deactivation due to the chloride treatments, Pd/SOMS exhibited resistance to chloride deactivation and metal leaching. The chloride treatments did not impact the textural properties of Pd/SOMS. The achieved deactivation resistance was attributed to the novel characteristics of the SOMS support.

1. Introduction

Hydrodechlorination is a solid-catalyzed chemical reaction where chlorinated hazardous compounds are converted to chloride-free hydrocarbons with a subsequent evolution of HCl. Although the HCl evolution from HDC reactions seems “innocent”, it has been reported that the catalytic performance of HDC catalysts is impacted by the unavoidable reaction product HCl. [1–8]. As HDC reaction takes place, the acidity of water increases due to the HCl evolution. When pH of the contaminated water is lower than the point of zero charge of the employed catalyst, the surface bears a positive charge that favors interactions of the anionic species, such as dissolved chlorides that can be found in water at high concentrations, with the positively-charged surface [1,9–12].

Interactions of chloride species with HDC catalysts result in several deactivation modes including formation of metal-chloride bonds [13–16], leaching of the active metal [1,17], and chloride-containing carbon deposition induced by acidity increase [6,15,18]. In addition, chloride species also promote sintering of Pd nanoparticles (NPs) [19], despite the fact that metal sintering is more pertinent to high temperature HDC reactions [13,18,19].

In order to mitigate the detrimental effects of chloride interactions, two types of approaches were reported in the literature to develop deactivation-resistant catalytic systems. In the first approach, the reaction product HCl was neutralized by adding bases such as NaOH, KOH to the reaction medium to control the pH [1,17,20,21]. Addition

* Corresponding author.
E-mail address: ozkan.1@osu.edu (U.S. Ozkan).

https://doi.org/10.1016/j.apcatb.2018.08.065
Received 5 June 2018; Received in revised form 17 August 2018; Accepted 23 August 2018
Available online 24 August 2018
0926-3373/

of bases to the reaction solution altered the catalytic activities in a pH-dependent manner [1,17,22]. After NaOH addition, if the resulting reaction solution is slightly acidic or neutral, catalytic activity increases were observed due to neutralization of HCl [1,17,23]. If the resulting solution is slightly basic or basic, however, catalytic activity decreases were observed since the basic reaction environment impaired the adsorption of the reactants on the catalytic surfaces [1,17]. When large volumes of contaminated water streams are considered, increasing pH of groundwater by external addition of NaOH may raise issues related to sustainability and practicality of the operation in groundwater applications [23–25]. Another way to control the solution pH is to use buffer solutions to maintain a non-acidic environment throughout the reaction [26]. It is, however, important to confirm that buffer solutions do not have a negative effect on the catalytic activity [27].

In the second approach, instead of controlling pH to neutralize HCl by external addition of base or buffer solutions, novel catalytic systems were designed to improve the deactivation resistance. Nutt et al. designed bimetallic Pd-Au nanoparticles (NPs) with a Pd-shell/Au-core structure [28,29]. The Pd-Au NPs exhibited a deactivation-resistance to chloride species obtained from NaCl, under reaction conditions where Pd/Al_2O_3 and Pd NPs deactivated. The poisoning resistance behavior was attributed to the electronic effects of Au on Pd [12]. Schuth et al. used a hydrophobic zeolite-Y to circumvent deactivation problems due to anionic species [30,31]. The hydrophobicity of the zeolite was altered by changing the Si/Al ratio. Significant poison-resistance was achieved against sulfite anions dissolved in water. The resistance to chloride poisoning, however, was not investigated in particular. Fritsch et al. developed a composite catalytic membrane system containing Pd active sites in hydrophobic polydimethylsiloxane [8]. In addition, Kopinke et al. coated Pd/Al_2O_3 catalyst with the same silicone polymer [32]. Although significant improvements were obtained against sulfite poisoning, catalytic deactivation due to chloride poisoning was observed in both cases [8,32]. In fact, the applied hydrophobic coating underwent silicone hydrolysis reactions and was degraded by HCl [33].

Our research group has been using a new class of silica-based materials, namely swellable organically-modified silica (SOMS), as an alternative catalyst scaffold to circumvent the deactivation issues of Pd-based HDC catalysts [34–37]. SOMS is a novel catalytic support with unique properties such as extreme hydrophobicity and high affinity for adsorbing organic compounds. SOMS also exhibits a swelling behavior upon contact with organic compounds [38–41]. The unique properties of SOMS allowed us to design “smart” catalytic materials in which the concentration of the active sites on the surface exhibits a stimuli-induced response where the stimulus is concentration of organics near the active sites [34]. Pd NPs incorporated to SOMS exhibited poison-resistant behavior in the presence of Li_2S for liquid-phase HDC of TCE. The deactivation resistance of Pd/SOMS to HCl poisoning was also demonstrated for gas-phase HDC of TCE [36] In addition, in-situ vibrational spectroscopy studies performed over Pd-incorporated SOMS showed that no observable carbon deposition occurred over Pd/SOMS while substantial amount of carbon formation occurred on Pd/Al_2O_3 during gas-phase HDC of TCE [35].

In this study, Pd/SOMS was investigated further for its resistance towards deactivation induced by chloride anions. Since the degree of deactivation depends on the concentration and the type of the poison or its precursor and the duration of poisoning, Pd/SOMS was exposed to chloride-containing aqueous solutions for the same duration with varied concentrations of two different chloride precursors, NaCl and HCl. In order to distinguish the effects of chloride deactivation from water soaking, treatments were also performed in the absence of chloride precursors in the treatment solution. Experiments were also performed over a benchmark HDC catalyst Pd/Al_2O_3 for comparison purposes.

2. Experimental

2.1. Catalyst synthesis

Edmiston and co-workers reported the synthesis procedure for SOMS previously [38–40,42]. SOMS was impregnated with Pd through incipient wetness impregnation (IWI) technique. The solution of Pd(II) acetate in acetone was added dropwise to the SOMS support until the support was saturated with the solution. This step was followed by drying at room temperature. Once a dry material was obtained, addition of Pd-containing solution was continued, until a 1% (weight) of Pd loading was achieved. The saturation-drying cycle was repeated until all the precursor solution was added to the SOMS support. Pd on SOMS was reduced with a solution of $NaBH_4$ in 95% ethanol. After reduction, Pd/SOMS particles were filtered, washed with ethanol, and dried at 70 °C.

1% Pd/Al_2O_3 catalyst was obtained from Sigma-Aldrich and reduced at 350 °C with 5%H_2/N_2.

2.2. Aqueous-phase chloride treatments

Pristine Pd/SOMS and Pd/Al_2O_3 catalysts were treated with aqueous solutions of NaCl and HCl at different concentrations at room temperature. Chloride treatments were conducted in a 0.5 l three-neck flask. Prior to He flushing, 0.35 g of pristine sample was placed in the flask and necks were sealed to obtain an air-tight environment. Once flushing was complete, 400 ml poisoning solution was added, and mixing was started. After 1 h of mixing, the solution was filtered. The resultant solid material was dried at 110 °C for one hour. The pH of the treatment solution was measured with a pH meter.

The aqueous-phase chloride treatment conditions were chosen as they relate to the treatment of contaminated groundwater where expected HCl concentration due to complete HDC of TCE is typically in ppm levels [10]. In our treatments, catalysts were exposed to chloride concentrations up to 0.1 M, providing an excessive driving force for the deactivation effects to be observed. Also, these conditions correspond to high molar ratios of chloride to Pd. For example this ratio is around 120 in 0.01 M HCl or NaCl solution,

2.3. Nitrogen physisorption

N_2 physisorption experiments were conducted on an accelerated surface area analyzer and porosimetry instrument (Micromeritics ASAP 2020). Samples were first degassed at 120 °C for 10 h under vacuum to remove moisture and impurities present on the sample. The analysis was conducted at 77 K. The surface area of catalysts was determined by the Brunauer–Emmett–Teller (BET) and the pore volume and pore size of the catalysts were determined by the Barrett-Joiner-Halenda (BJH) method. The pore size distribution was extracted from the desorption isotherm by the BJH method.

2.4. Inductively coupled plasma – optical emission spectrometry (ICP-OES)

Amount of Pd leached to the treatment solution was analyzed by ICP-OES. After the chloride treatments, the treatment solution was filtered using a syringe filter and then was subjected to elemental analysis for measuring the concentration of leached Pd. This was carried out using a Perkin- Elmer Optima 4300DV ICP-OES.

2.5. X-ray photoelectron spectroscopy (XPS)

A Kratos Ultra Axis Spectrometer equipped with a monochromatized Al Kα X-ray source operating at 12 kV and 10 mA was used to acquire XPS spectra of pristine and treated samples of Pd/SOMS and Pd/Al_2O_3. Powder samples were loaded on the carbon tape and placed in the XPS chamber. After evacuating overnight, a survey scan followed

by high resolution region scans were collected. The charging effects were corrected with respect to C 1 s (284.5 eV). Atomic ratios of surface elements were calculated after correcting the XPS signal intensities by using atomic sensitivity factors. CasaXPS software was used to perform carbon-calibration and peak fitting of the data.

2.6. Extended X-ray absorption fine structure (EXAFS)

Pd-K edge (24.350 keV) X-ray absorption fine structure (XAFS) measurements of pristine and HCl- or NaCl-treated samples of Pd/Al_2O_3 and Pd/SOMS in transmission mode were conducted on the insertion device beamline of the Materials Research Collaborative Access Team (MRCAT-10ID) at Advanced Photon Source at Argonne National Laboratory [43]. The samples were loaded into a cylindrical sample holder consisting of six wells. The energy spectra were normalized and Fourier transform scattering magnitudes were obtained by a standard protocol using WINXAS 3.2 [44]. The energy alignment was performed with respect to the simultaneously collected XAFS spectrum of a Pd foil. Edge energy was determined from the first derivative of the spectra. Phase shifts and backscattering amplitudes were obtained experimentally from EXAFS spectra of Pd foil for Pd-Pd (12 at 2.75 Å), palladium oxide for Pd-O (4 at 2.05 Å), and palladium chloride for Pd-Cl (4 at 2.31 Å). The EXAFS coordination parameters (R: interatomic bond distance and N: coordination number) were obtained by a least-square fit in R-space and k-space of the nearest neighbor.

2.7. DRIFTS of adsorbed CO

CO adsorption-desorption experiments were performed using in situ diffuse reflectance Fourier transform spectroscopy (DRIFTS) over pristine and HCl- or NaCl-treated samples of Pd/Al_2O_3 and Pd/SOMS. Thermo NICOLET 6700 FTIR spectrometer equipped with a cryogenic MCT detector and KBr beam splitter was used. Powder samples were grinded and loaded into the sample chamber of an in-situ reaction cell (Harricks – Praying Mantis). Before spectral acquisition, the cell was flushed and the samples were pretreated at 110 °C under He. The temperature was reduced to 40 °C and a background spectrum was collected before introducing CO into the cell. Following saturating the samples with CO, weakly bound species were removed by helium and the spectra were acquired. The background spectra were subtracted from sample spectra by using OMNIC 8.1 software.

2.8. Catalytic activity experiments

Aqueous-phase HDC of TCE experiments were performed over pristine and HCl- or NaCl-treated Pd/SOMS and Pd/Al_2O_3 catalysts at 50 bar and 30 °C in a batch reactor. Catalysts in powder form were loaded into the catalyst addition device. The reactor was filled with 200 ml of TCE solution and then sealed, tightened, and placed in the reactor assembly. Before starting the reaction, the reactor was flushed with He. It took around 30 min for the temperature to stabilize. Once the temperature was stable at 30 °C, the reactor was pressurized with H_2 up to 50 bar to ensure the presence of excess H_2. In addition, pure hydrogen was present in the headspace of the reactor forming a sufficient reservoir. At time = 0, a liquid sample was taken, which was used to determine the initial concentration of TCE. At time zero, the concentration of TCE was found to be approximately 250 ppm. After the liquid sample was taken, the catalyst addition device was activated, and the reaction started. Liquid samples were taken throughout the reaction at periodic intervals and analyzed using a high-performance liquid chromatograph (HPLC) equipped with a UV/Vis detector (Shimadzu, SPD-20A) and selective chloride electrode (Cole Palmer, UX-27504-08). The HPLC was operated in binary-mode and reverse-phase where the mobile phase underwent gradient elution to 95:5 acetonitrile and water during the analysis of samples. Analysis, separation, and quantification of unconverted educts and Cl-containing products including chlorinated ethanes and ethylenes were achieved with the help of a 5 µL injection loop, an injection valve, and C18 column. Tetrahydrofuran was used as an internal standard. The mass balance of the system was ensured by performing a chloride balance. A satisfactory chloride balance of 96% or higher was obtained indicating the absence of significant loss of volatile chloride-containing compounds during the reaction and the sampling.

The absence of external and internal mass transfer limitations was demonstrated by a combination of experiments and calculations [45]. Briefly, HDC of TCE experiments were performed at different stirring speeds and using Pd/SOMS with different particle sizes. The reaction parameters during these experiments were kept constant. The diffusion scale of the system was minimized by working with powder samples with an average particle diameter less than 74 µm (200 mesh). The reactor was continuously stirred at 2000 rpm to the eliminate mass transfer limitations. The absence of mass transfer limitations was also verified by using the well-established criteria in the literature, which entailed calculating Wagner modulus for best performing catalyst since the extent to which mass transfer limitations exist will be maximum when the catalytic activity is the highest. Wagner modulus calculated for the first 40 min of the reaction, where the reaction rate is the highest, turned out to be significantly smaller than 0.15. This verifies that the mass transfer limitations due to pore diffusion are absent in our batch reactor [46]. The thermal effects of the reaction were also investigated. At full conversion of TCE, the adiabatic temperature rise was found to be less than 0.2 °C. In addition, the activity experiments were also performed under a He atmosphere, i.e., without H_2, to examine the TCE uptake by the catalyst/support. No significant TCE uptake was observed that would mask the catalytic performance.

3. Results and discussion

In an attempt to establish a relationship between the changes in catalyst properties and in the catalytic activity due to chloride treatments, several characterization studies including N_2 physisorption, ICP-OES, XPS, EXAFS, and DRIFTS of adsorbed CO were performed over pristine and treated samples of Pd/SOMS and Pd/Al_2O_3. NaCl and HCl were chosen for these treatments due to their relevance to HDC reactions in which HCl is the primary reaction product.

3.1. Nitrogen physisorption

Nitrogen physisorption experiments were performed to examine the textural properties of Pd/SOMS and Pd/Al_2O_3 and the changes therein upon exposure to chloride-containing solutions. Pd/Al_2O_3 and Pd/SOMS catalysts were treated with 0.1 M NaCl and 0.1 M HCl as described in the experimental section. Nitrogen adsorption-desorption isotherms and pore size distribution plots of pristine and treated Pd/Al_2O_3 are shown in Fig. 1a. The pristine Pd/Al_2O_3 exhibited type-IV adsorption isotherm with H3-type hysteresis caused by capillary condensation of nitrogen [47]. Upon exposure to chloride solutions, a significant decrease in the quantity of adsorbed nitrogen was observed. In addition, the pore size distribution of pristine Pd/Al_2O_3 shifted to lower pore diameters.

The adsorption-desorption isotherm of Pd/SOMS, shown in Fig. 1b, exhibited characteristics of mesoporous materials with type-IV adsorption isotherm and H2-type hysteresis caused by capillary condensation. In addition, another type of hysteresis was observed due to swellable nature of Pd/SOMS at lower relative pressures between 0.1 and 0.4 [47,48]. Although the pore size distribution shows that SOMS has a bimodal porous structure, the peak at 3.7 is an artifact of nitrogen physisorption and does not result from the existence of real pores [49]. Chloride treatments did not have an effect on the adsorption-desorption isotherms, the type of hysteresis, and the pore size distribution. The hysteresis observed due to swellable nature of Pd/SOMS was not affected from these treatments, suggesting that the swelling characteristic

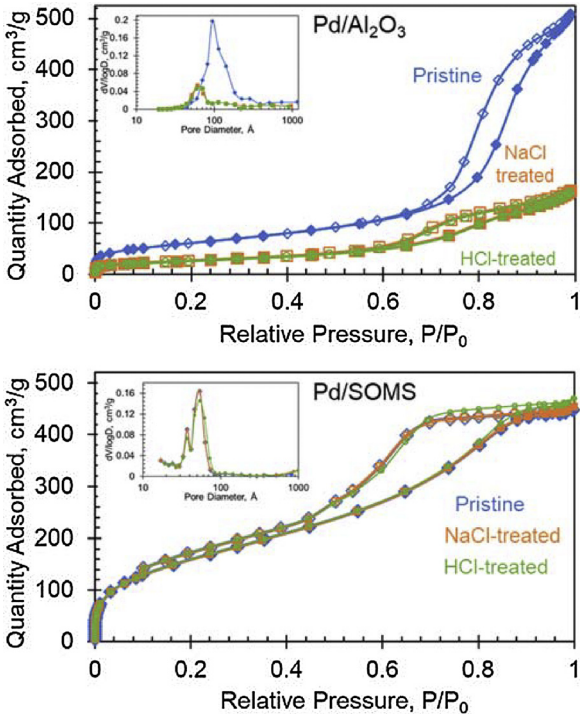

Fig. 1. Nitrogen adsorption-desorption isotherms of pristine, 0.1 M NaCl-treated, and 0.1 M HCl-treated Pd/Al_2O_3 and Pd/SOMS. Insets: BJH pore size distributions.

of Pd/SOMS was retained.

BET surface area, BJH pore volume, and BJH pore diameter of pristine and HCl- or NaCl-treated Pd/Al_2O_3 are tabulated in Table 1. BET surface area for pristine Pd/Al_2O_3 decreased significantly upon treatments with NaCl and HCl solutions, going down from 220 m^2/g to 95-98 m^2/g. Pore volume and pore diameter values of pristine Pd/Al_2O_3 decreased as well. The pore volume decreased from 0.79 cc/g to 0.25-0.26 cc/g and pore diameter decreased from 10.3 nm to 7.4–7.5 nm.

To distinguish the effect of chloride treatment from the effect of water-soaking, N_2 physisorption was performed over water-soaked Pd/Al_2O_3. As shown in Table 1, textural properties of water-soaked and HCl- or NaCl-treated Pd/Al_2O_3 were not different. The results show that the changes in the textural properties due to the chloride treatments originated from interactions of Pd/Al_2O_3 with water, rather than interactions of Pd/Al_2O_3 with chloride ions. It is suspected that the hydration of the surface of Pd/Al_2O_3 resulted in this behavior. To remove the surface hydration on water-soaked Pd/Al_2O_3, a higher degassing temperature was employed prior to N_2 physisorption. Water-soaked Pd/Al_2O_3 was degassed at 200 °C instead of 120 °C. However, no significant effects were observed on the textural properties. BET surface area, pore volume, and pore diameter of water-soaked Pd/Al_2O_3 degassed at

Table 1
Textural properties of pristine, water-soaked, NaCl-treated, and HCl-treated Pd/Al_2O_3 and Pd/SOMS.

Samples		BET Surface Area, m^2/g	Pore Volume, cc/g	Pore Diameter, nm
Pd/Al_2O_3	Pristine	220	0.79	10.3
	Water-soaked	97	0.25	7.4
	0.1 M NaCl	98	0.26	7.4
	0.1 M HCl	95	0.25	7.5
Pd/SOMS	Pristine	590	0.73	3.9
	Water-soaked	604	0.75	3.9
	0.1 M NaCl	590	0.74	4.0
	0.1 M HCl	591	0.73	4.3

Table 2
Percentages of Pd leached from Pd/Al_2O_3 and Pd/SOMS after chloride treatments.

Treatments	pH	% Pd Leaching	
		Pd/Al_2O_3	Pd/SOMS
0.1 M NaCl	6.6	< 1	< 1
0.01 M HCl	2.1	76	< 1
0.1 M HCl	1.2	83	3
0.1 M $HClO_4$	1.1	3	1

200 °C were found to be 100 m^2/g, 0.28 cc/g, and 7.8 nm, respectively. The surface hydration over Pd/Al_2O_3 has been reported to be difficult to remove, and temperatures as high as 900 °C may be needed for the complete removal of hydroxyls originating from the surface hydration [50,51].

The textural properties of pristine, water-soaked, and chloride-treated Pd/SOMS catalysts are given in Table 1. BET surface area, BJH pore volume, and BJH pore diameter of pristine Pd/SOMS were 590 m^2/g, 0.73 cc/g, and 3.9 nm, respectively. The textural properties of Pd/SOMS were not affected from the chloride treatments, because of the hydrophobic nature of Pd/SOMS limiting the extent of the surface hydration.

3.2. Inductively coupled plasma – optical emission spectrometry (ICP-OES)

In order to see if there was any metal leaching from Pd/Al_2O_3 and Pd/SOMS because of chloride treatments, experiments were run where the liquid samples were taken from the treatment solutions, filtered, and analyzed by ICP-OES. The percentages of Pd leached from Pd/Al_2O_3 and Pd/SOMS are shown in Table 2. Treating Pd/Al_2O_3 with 0.1 M NaCl solution did not lead to any Pd leaching. Treating Pd/Al_2O_3 with 0.01 M HCl, however, leached ~76% of Pd. When the chloride treatment experiments were performed over Pd/SOMS, a high resistance to leaching was observed. Treating Pd/SOMS with 0.1 M NaCl or 0.01 M HCl did not cause Pd to leach into the treatment solution.

It is expected that metallic Pd NPs present in the pristine Pd/Al_2O_3 were stabilized in Pd^{2+} state by the formation of Cl-containing Pd complexes in the presence of the chloride ion-containing solutions. Although, as seen in the EXAFS results presented in Section 3.4, Pd-chloride complexes were formed on alumina when exposed to 0.1 M NaCl solution, no leaching was observed. This may be because of the lower solubility of chlorinated Pd complexes in the NaCl solution which had a neutral pH.

Although 0.1 M NaCl and 0.1 M HCl contain the same concentration of chloride ions, the extent of leaching over Pd/Al_2O_3 was significantly higher under acidic conditions. If the acidity of the treatment solution is increased, the chlorination of Pd NPs is followed by leaching, since Pd^{2+} species stabilized by chloride is highly soluble under acidic conditions [52]. It was reported that the solubility of such species increased by four orders of magnitude when the pH of the treatment solution was decreased from 7 to 4 in the presence of 0.1 M Cl^--containing solution [27,52]. Therefore, leaching is likely to occur because of solubility increase of Pd-Cl complexes under acidic conditions.

To elucidate the role of the acidity further, chloride treatment experiments were performed with 0.1 M $HClO_4$ solution. Treatment with 0.1 M $HClO_4$, however, resulted in leaching of only 3% of Pd from Pd/Al_2O_3. It is conceivable that because perchlorate ion, due to its lower charge density, is not as strong a ligand as chloride, it does not lead to the formation of chlorinated Pd complexes in this medium. This may explain the low level of leaching observed in the perchlorate solution although the medium was highly acidic.

Leaching of the active metal is an important problem in liquid-phase chemical reactions since the leached metal in a flow reactor will be flushed out. This would not only cause irreversible loss of the active

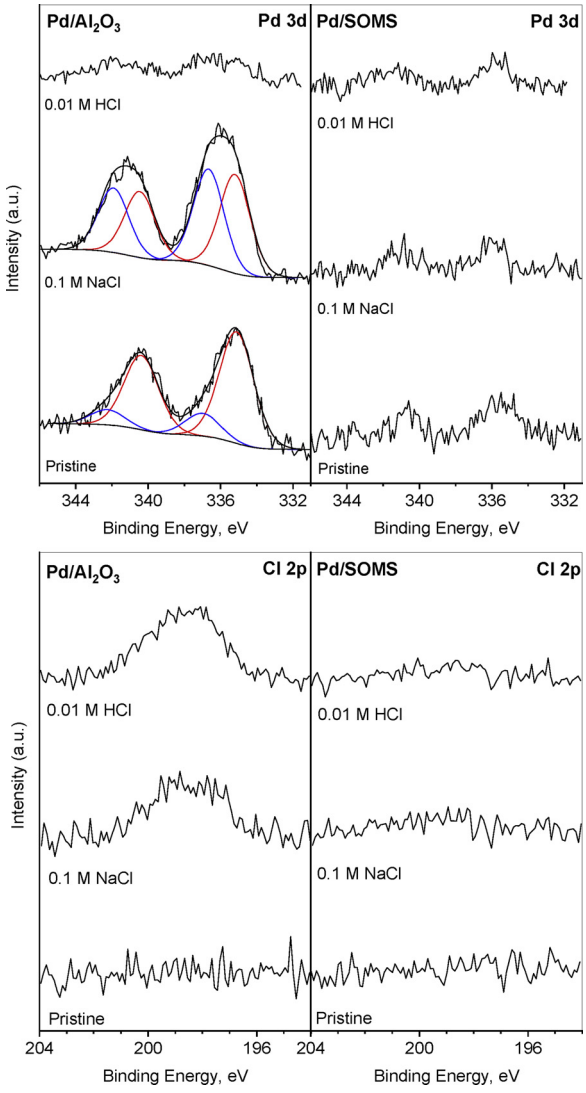

Fig. 2. Pd 3d and Cl 2p XPS spectra of pristine, NaCl-treated, and HCl-treated Pd/Al_2O_3 and Pd/SOMS.

element from the catalyst, but also be harmful to humans and ecosystems. The leached metal may also exhibit catalytic activity when it is still in contact with the reactants after leaching. To test whether the leached metal has catalytic activity for HDC of TCE, a portion of the chloride treatment solution of Pd/Al_2O_3 with 0.01 M HCl was used in the reactor since it contained leached Pd. Activity experiments were performed at 50 bar and 30 °C without any additional catalyst. The amount of leached Pd in the reaction medium was set to be equivalent to the amount Pd in the activity experiments presented in Section 3.6. No TCE conversion was observed, indicating that Pd leached due to HCl was not active for aqueous-phase HDC of TCE.

3.3. X-ray photoelectron spectroscopy

XPS studies over Pd/Al_2O_3 and Pd/SOMS in their pristine and treated states were performed to examine the changes on the surface due to chloride-treatments. Fig. 2 shows Pd 3d and Cl 2p XPS spectra of pristine, 0.1 M NaCl-treated, and 0.01 M HCl-treated samples of Pd/Al_2O_3 and Pd/SOMS.

The Pd $3d_{5/2}$ peak of Pd/Al_2O_3 is a broad peak positioned at a binding energy of 335.6 eV, which is between the binding energy of metallic palladium (335–335.2 eV) and oxidized palladium (336.3–337.2) [14,53–55]. To obtain the oxidation state of surface Pd,

Table 3
XPS results obtained for pristine and treated Pd/Al_2O_3.

Sample	Binding Energy, eV		Pd^{2+}/Pd°	Cl/Al
	Pd° $3d_{5/2}$	Pd^{2+} $3d_{5/2}$		
Pd/Al_2O_3 – Pristine	335.1	337.0	0.2	0
Pd/Al_2O_3 – 0.1 M NaCl	335.2	336.7	1.0	0.01
Pd/Al_2O_3 – 0.01 M HCl	–	–	–	0.02

the spectrum was deconvoluted. Pd $3d_{5/2}$ and $3d_{3/2}$ peaks were fitted to a doublet with a spin-orbit splitting ratio of 3:2 and a fixed doublet separation of 5.26 eV [56]. The binding energies of Pd° $3d_{5/2}$ and Pd^{2+} $3d_{5/2}$ peaks are given in Table 3. It was found that 83% of surface Pd was metallic and the remaining 17% was oxidized at an oxidation state of 2+, resulting in a Pd^{2+}/Pd° ratio of 0.2.

Treatment with 0.1 M NaCl solution caused overall XPS spectra to shift to higher binding energies indicating the increase in the oxidation state of Pd on Pd/Al_2O_3. The deconvolution results (Table 3) revealed that 51% of surface Pd was metallic and the remaining 49% was oxidized with an oxidation state of +2. After treating Pd/Al_2O_3 with 0.1 M NaCl, the Pd^{2+}/Pd° ratio increased from 0.2 to 1.0. The increase in the oxidation state of Pd was attributed to the stabilization of Pd in +2 state due to the formation of Cl-containing Pd complexes [54,55].

HCl treatment caused more substantial changes on the Pd 3d spectrum of Pd/Al_2O_3. The most obvious change was the loss of intensity due to lower amount of Pd present in the treated catalyst. ICP-OES results presented in Section 3.2 showed that 76% of Pd leached after treating Pd/Al_2O_3 with 0.01 M HCl. Since the spectrum of Pd/Al_2O_3 treated by 0.01 M HCl has a low signal to noise ratio, the deconvolution was not performed.

The Pd 3d spectra of pristine and chloride-treated samples of Pd/SOMS are shown in Fig. 2. Since Pd metal particles were deposited inside the swollen matrix of SOMS during synthesis, a weak Pd signal was obtained in Pd 3d region [34]. To examine the changes in the state of Pd NPs, X-ray absorption spectroscopy experiments were performed and will be presented later in the paper.

As shown in Fig. 2, the chloride treatment with NaCl or HCl solution resulted in a peak to appear on the Cl 2p spectrum of Pd/Al_2O_3 due to accumulation of chloride-containing species. The peaks seen in Fig. 2 possibly stemmed from the presence of adsorbed chloride ions and some Pd-chloride complexes on the surface [57–60].

Atomic ratios of surface elements were calculated after correcting the XPS signal by using atomic sensitivity factors [56]. The Cl/Al ratios obtained over pristine and chloride treated Pd/Al_2O_3 are presented in Table 3. The Cl/Al ratio obtained over HCl-treated Pd/Al_2O_3 was higher than the ratio obtained over NaCl-treated Pd/Al_2O_3. The difference in the Cl/Al ratio suggests that the extent of accumulation of chloride species in HCl treatment was higher although the concentration of chloride anions was an order of magnitude lower. This could also be due to chloride ions adsorbing on the alumina surface in the HCl solution since at low pH, the surface charge on alumina would be reduced, potentially leading to chloride adsorption.

Cl 2p spectra of pristine and treated Pd/SOMS samples, shown in Fig. 2, did not exhibit any signal associated with chloride species. This is an important finding to demonstrate that the chloride species did not adsorb on the surface of Pd/SOMS.

3.4. Extended X-ray absorption fine structure (EXAFS)

In order to examine the changes in the local atomic environment of Pd due to chloride treatments, X-ray absorption experiments at Pd-K edge were performed over pristine and treated samples of Pd/Al_2O_3 and Pd/SOMS. The k2-weighted Fourier transform (FT) magnitudes and EXAFS coordination parameters are given in Fig. 3 and Table 4.

The pristine Pd/Al_2O_3 exhibited Pd-Pd and Pd-O scatterings with

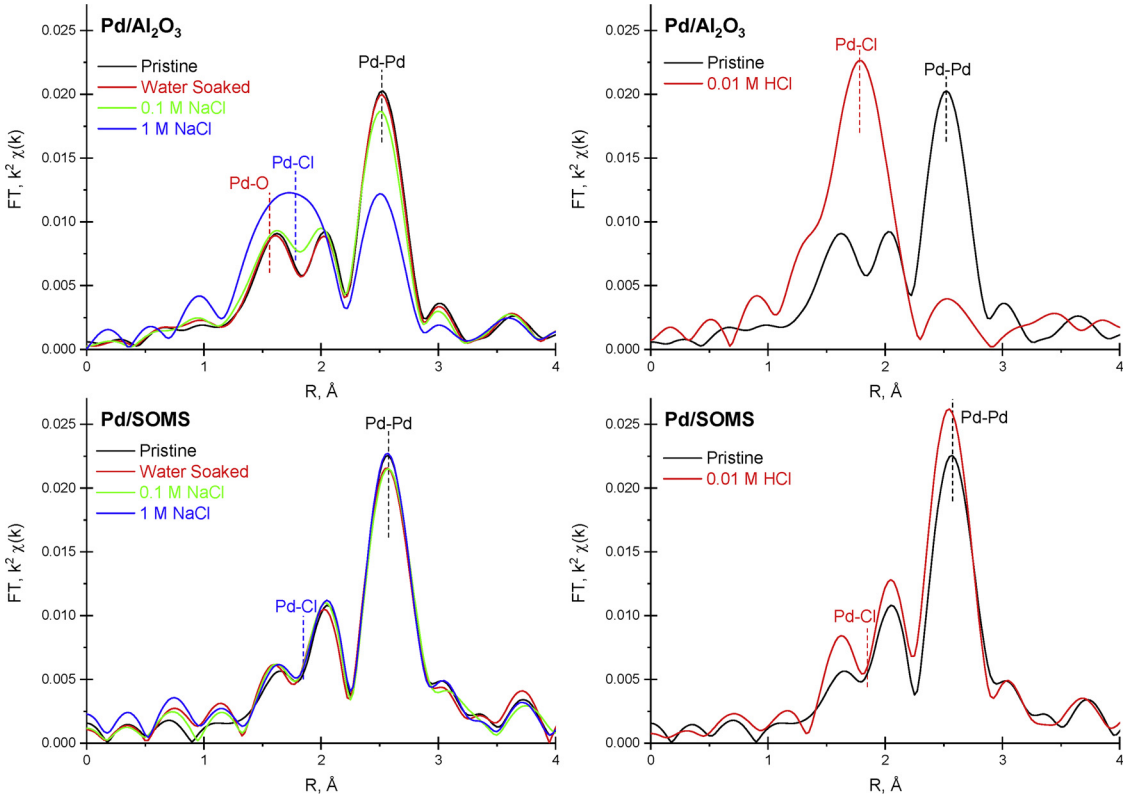

Fig. 3. The k2-weighted FT magnitudes of pristine, water-soaked, HCl-treated, and NaCl-treated Pd/Al_2O_3 and Pd/SOMS.

Table 4
Pd K-edge EXAFS fitting results for pristine, water-soaked, NaCl-treated, and HCl-treated samples of Pd/Al_2O_3 and Pd/SOMS (k^2: Δk = 2.9–12.1 $Å^{-1}$, ΔR = 1–3 Å; N ± 10%, R ± 0.02 Å).

Sample		XANES Energy, keV	Scatter	N	R, Å	$\Delta\sigma^2$ (10^3)	Eo, eV
Pd/Al_2O_3	Pristine	24.3518	Pd-Pd	6.5	2.74	2.0	−2.4
			Pd-O	1.4	2.05	2.0	1.6
	Water Soaked	24.3529	Pd-Pd	6.4	2.74	2.0	−3.6
			Pd-O	1.4	2.05	2.0	0.8
	0.1 M NaCl	24.3540	Pd-Pd	6.0	2.74	2.0	−4.5
			Pd-O	1.4	2.05	2.0	2.5
			Pd-Cl	0.3	2.31	2.0	0.9
	1 M NaCl	24.3544	Pd-Pd	4.0	2.74	2.0	−5.3
			Pd-O	1.4	2.05	2.0	−2.8
			Pd-Cl	1.3	2.31	2.0	2.8
	0.01 M HCl	24.3541	Pd-Cl	3.8	2.29	2.0	−0.4
Pd/SOMS	Pristine	24.3501	Pd-Pd	9.9	2.76	4.0	−1.1
	Water Soaked	24.3500	Pd-Pd	9.5	2.75	4.0	−1.2
	0.1 M NaCl	24.3500	Pd-Pd	9.6	2.76	4.0	−0.8
	1 M NaCl	24.3551	Pd-Pd	9.9	2.76	4.0	−1.1
	0.01 M HCl	24.3502	Pd-Pd	9.8	2.74	2.8	−1.1

coordination numbers of 6.5 and 1.4, respectively. Since there are 4 Pd-O bonds in fully oxidized PdO, a coordination number of 1.4 for Pd-O indicates that there is about 35% Pd(II). In addition, since 65% of the Pd is metallic, the true Pd-Pd coordination number is 10.0 [61]. This indicates that Pd NPs on pristine Al_2O_3 were slightly oxidized. Soaking Pd/Al_2O_3 in water did not result in any changes in the coordination environment of Pd. The coordination environment of Pd NPs on Al_2O_3, however, changed upon treatment with NaCl solution. With increasing NaCl concentration of the solution from 0.1 M to 1 M, the coordination number of Pd-Cl scattering was increased from 0.3 to 1.3 with a corresponding decrease of Pd-Pd scattering from 6.0 to 4.0, as shown in Table 4. As expected, increasing the concentration of NaCl resulted in more severe poisoning due to a greater driving force.

Pd/Al_2O_3 treated by 0.01 M HCl was also characterized by EXAFS spectroscopy. It should be noted that EXAFS probed the nature of Pd NPs remaining on Pd/Al_2O_3 after leaching since the treatment resulted in a loss of 76% of Pd, as explained in Section 3.2. This is why a lower edge jump was obtained on the HCl-treated Pd/Al_2O_3. The FT magnitude of HCl-treated Pd/Al_2O_3, shown in Fig. 3b, revealed the presence of only Pd-Cl scattering, indicating that Pd remaining on Pd/Al_2O_3 after leaching consisted mainly of chlorinated Pd complexes. The fitting results showed that the coordination number of Pd-Cl scattering on HCl-treated Pd/Al_2O_3 was 3.8. This sample has very little metallic Pd NPs remaining.

The FT magnitude and EXAFS coordination parameters of pristine Pd/SOMS are shown in Fig. 3 and Table 4, respectively. The pristine Pd/SOMS is composed of only Pd-Pd scattering indicating that Pd NPs incorporated into SOMS are in metallic state with a coordination number of 9.9.The interatomic bond distance of Pd in Pd/SOMS was found to be slightly larger than that of Pd foil (2.75 Å), possibly due to the formation of Pd-H species [62,63]. The formation of Pd-H is likely to occur in the presence of H_2 that evolves during $NaBH_4$ reduction step of the synthesis. Unlike the Pd/Al_2O_3, there is little oxidized Pd(II) in the Pd/SOMS under similar conditions.

Soaking Pd/SOMS in water did not result in any significant changes in the coordination environment of Pd. The observed changes in the fitting results, shown in Table 4, are within the experimental uncertainty of EXAFS fitting. In addition, the Pd-Pd metallic scattering magnitudes and EXAFS coordination parameters of the pristine and NaCl-treated samples remained unchanged, indicating that chloride anions were not able to enter the atomic environment of Pd during treatment with NaCl.

The FT magnitude of Pd/SOMS treated with 0.01 M HCl is also

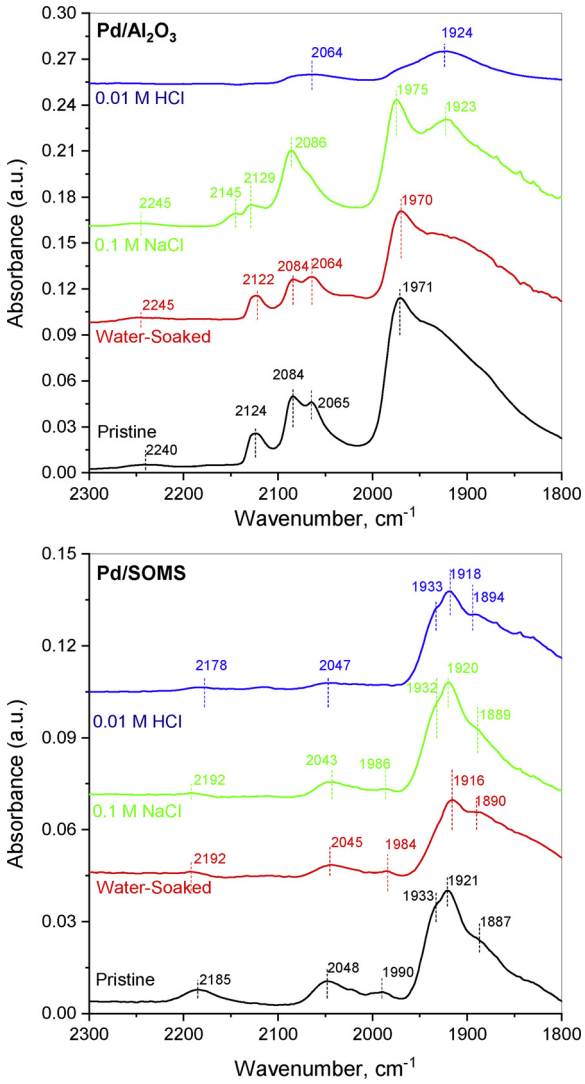

Fig. 4. DRIFTS spectra of CO adsorbed on pristine, water-soaked, NaCl-treated, and HCl-treated Pd/Al_2O_3 and Pd/SOMS after flushing with He.

shown in Fig. 3. It should be noted that the amount of Pd in pristine and HCl-treated Pd/SOMS were similar after exposure to 0.01 M HCl solution since no leaching was observed over Pd/SOMS. Treating Pd/SOMS with 0.01 M HCl solution resulted in a decrease in the interatomic distance of Pd NPs from 2.76 Å to 2.74 Å. Although the magnitude of the decrease in the interatomic distance of Pd-Pd is still within the experimental uncertainty, this decrease could be attributed to removal of H from Pd-H as a result of HCl-treatment [62,63]. Nevertheless, Pd-Cl scattering was found to be absent in Pd/SOMS treated by 0.01 M HCl, as shown in Fig. 3. These results demonstrate the deactivation-resistant nature of Pd/SOMS to chloride anions under acidic conditions.

3.5. DRIFTS of adsorbed CO

The nature of Pd particles in pristine and treated catalysts was examined by in situ diffuse reflectance infrared Fourier transform spectroscopy (DRIFTS). Carbon monoxide was chosen as a probe molecule to investigate the properties of Pd and how these properties were affected by chloride treatments.

DRIFTS spectra for pristine, water-soaked, NaCl-treated, and HCl-treated Pd/Al_2O_3 in the 2300-1800 cm^{-1} range are shown in Fig. 4. The pristine Pd/Al_2O_3 spectrum has five bands at 2240 cm^{-1}, 2124 cm^{-1}, 2084 cm^{-1}, 2065 cm^{-1}, and 1971 cm^{-1}. The band at 2240 cm^{-1} was ascribed to CO adsorbed on coordinatively unsaturated (cus) Al^{3+} ions [64]. Among the remaining four bands, the bands above 2000 cm^{-1} correspond to linearly-bound adsorbed CO, whereas the bands below 2000 cm^{-1} correspond to bridged adsorbed CO [64–68]. The 2124 cm^{-1} band was ascribed to linearly adsorbed CO on cationic Pd, indicating that Pd NPs on Pd/Al_2O_3 are slightly oxidized [64,68]. The 2084 cm^{-1} and 2065 cm^{-1} bands were ascribed to linearly adsorbed CO on metallic Pd ($Pd^{\circ}-CO$) [66,67]. The 1971 cm^{-1} band with a shoulder around 1939 cm^{-1} was assigned to bridged adsorbed CO on Pd (Pd_x-CO) [67–69]. At lower wavelengths around 1880 cm^{-1}, there was still some contribution to IR absorbance that originated from three-fold isolated bridged CO [64–66,68].

The IR spectrum of water-soaked Pd/Al_2O_3 was similar to that of pristine Pd/Al_2O_3 except three main features. The first difference is that the intensity of IR spectrum of water-soaked Pd/Al_2O_3 was lower than that of pristine Pd/Al_2O_3. This could be associated with the coverage of the surface with hydroxyl ions due to interactions of water with Pd/Al_2O_3. After soaking in water, Pd/Al_2O_3 was dried to remove hydroxyl coverage on the surface. In addition, another pretreatment step was employed before CO adsorption. Complete removal of hydroxyl ions, however, requires very high pretreatment temperatures [50,51]. Such high pretreatment temperatures were avoided in this study so as not to modify the electronic structure of Pd NPs due to the pretreatment since the aim of the study is to observe the differences on Pd properties due to chloride treatments. The second difference is that there was a minor shift in the positions of the IR bands towards lower wavenumbers. This could be a consequence of water soaking that made dipole - dipole interactions between neighboring CO molecules weaker [66]. The third difference is the change of relative intensity of the 2084 cm^{-1} band to that of the 2064 cm^{-1}. Unlike the pristine Pd/Al_2O_3, the IR spectrum of water-soaked Pd/Al_2O_3 showed that the 2064 cm^{-1} band was as strong as the 2084 cm^{-1} band. This was attributed to minor changes of electronic properties of Pd due to water-soaking.

Overall, water soaking did not change the properties of Pd significantly. Treatment with 0.1 M NaCl solution, however, caused formation of new IR bands at 2145 cm^{-1} and 1923 cm^{-1}. The former band was ascribed to interactions of chlorinated Pd with CO [69] while the latter band was attributed to the formation of chlorocarbonyl complexes on Pd/Al_2O_3 where Pd was stabilized at an oxidation state of 1 + by neighboring chlorides [64]. The 2084 cm^{-1} and 2064 cm^{-1} bands observed in pristine and water-soaked Pd/Al_2O_3 appeared as a single band at 2086 cm^{-1}, suggesting that there were changes in the nature of Pd due to exposure to NaCl solution. According to Agostini et al. [70], these changes are mostly due to modifications of Pd properties due to poisoning rather than morphological changes [70].

The IR spectrum of HCl-treated Pd/Al_2O_3 exhibited several differences from that of pristine Pd/Al_2O_3. The intensity of the spectrum was markedly lower since HCl treatment caused leaching of significant amount of Pd. In addition, CO interactions with Pd resulted in disappearance of the band at 2245 cm^{-1} that originated from coordinatively unsaturated (cus) Al^{3+} ion [64] and appearance of a new band at 1924 cm^{-1} due to formation of chlorocarbonyl complexes on Pd/Al_2O_3 [64,66,67].

DRIFTS of adsorbed CO was also studied over pristine and treated samples of Pd/SOMS. As shown in Fig. 4, six IR bands were observed at 2185 cm^{-1}, 2048 cm^{-1}, 1990 cm^{-1}, 1933 cm^{-1}, 1921 cm^{-1}, and 1887 cm^{-1} over pristine Pd/SOMS. The band at 2185 cm^{-1} is at too high a wavenumber to be considered as linearly adsorbed CO on oxidized Pd [60,65,66]. This band was ascribed to the interactions of CO with the support. The band at 2048 cm^{-1} was rather a broad band and attributed to linearly-bound adsorbed CO on Pd [66,68,71–73]. The bands below 2000 cm^{-1} were ascribed to bridged adsorbed CO on Pd [64–68]. CO adsorption on Pd/SOMS did not result in a strong IR band at 1990 cm^{-1} which is typically attributed to twofold bridged CO [64–68]. It, however, resulted in three-fold IR bands as evidenced by the bands at 1933 cm^{-1} and 1921 cm^{-1} [66,69,74].

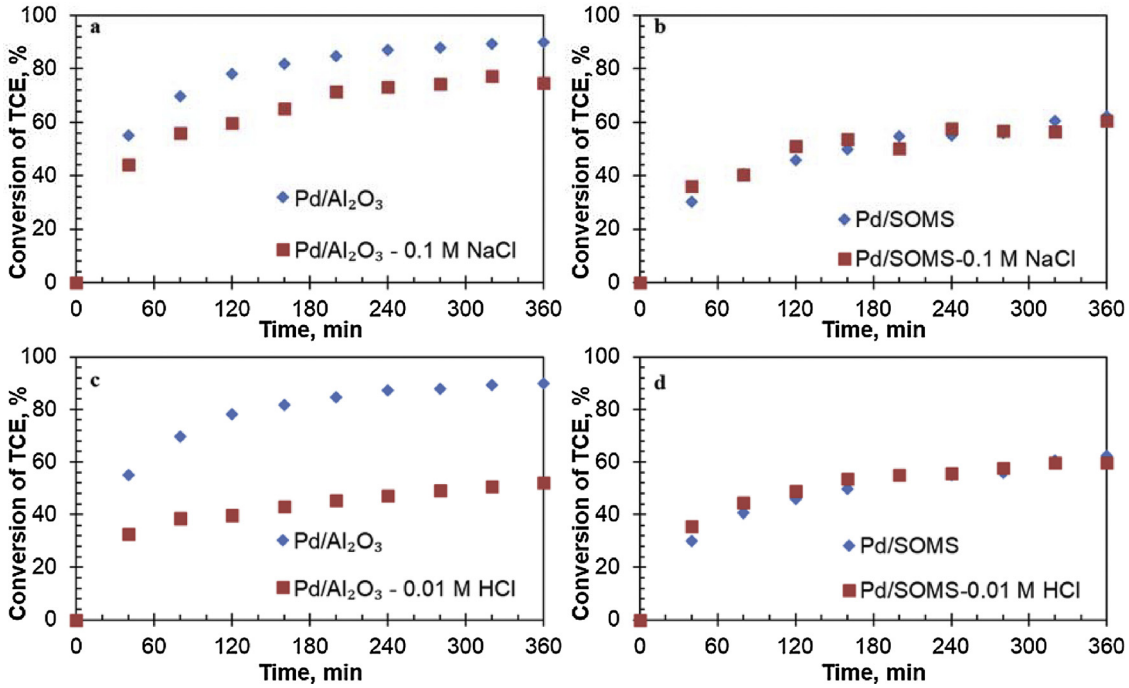

Fig. 5. Comparison of catalytic activities over pristine and treated Pd/Al_2O_3 and Pd/SOMS. (a) and (b) Effect of 0.1 M NaCl, (c) and (d) Effect of 0.01 M HCl. Reaction Conditions: 50 bar, 30 °C, 0.025 (mgcat)/(ml solution), $[TCE]_0$ = 250 ppm.

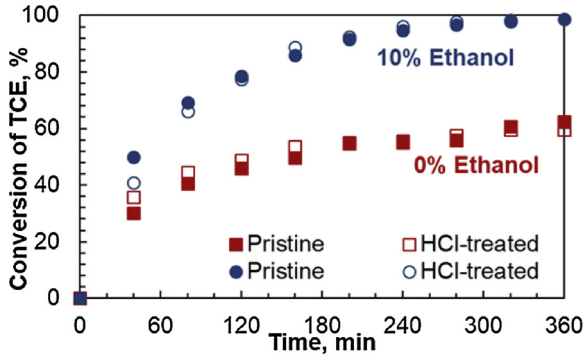

Fig. 6. Catalytic activity data showing TCE conversion with respect to time over pristine and HCl-treated Pd/SOMS in the absence and presence of 10% ethanol in the reaction medium. Reaction Conditions: 50 bar, 30 °C, 0.025 (mgcat)/(ml solution), $[TCE]_0$ = 250 ppm, $[Ethanol]_0$ = 0% or 10%.

The IR spectrum of adsorbed CO on pristine and treated Pd/SOMS showed that aqueous-phase treatments including water soaking did not cause significant changes on the properties of Pd. For instance, the intensity decrease observed over water-soaked Pd/Al_2O_3 in comparison to its pristine catalyst was not observed over water-soaked Pd/SOMS. Being a hydrophobic material, Pd/SOMS does not adsorb as much water as Pd/Al_2O_3 [36]. As a result, the intensity changes associated with surface hydration were negligible. In addition, treating Pd/SOMS with 0.1 M NaCl or 0.01 M HCl did not display bands associated with Pd-Cl interactions [64,69,70]. In the spectra of treated Pd/SOMS, there were, however, several minor differences in the IR band positions presumably because of changes in dipole-dipole interactions.

3.6. Catalytic activity experiments

The pristine and treated states of Pd/Al_2O_3 and Pd/SOMS catalysts were tested for aqueous-phase HDC of TCE at 50 bar and 30 °C. TCE conversions obtained over pristine catalysts are given in Fig. 5. Pd/Al_2O_3 exhibited better catalytic activity than Pd/SOMS throughout the reaction on the basis of equal Pd amount in the reactor. TCE conversions obtained over Pd/Al_2O_3 and Pd/SOMS at the end of six hours were 89% and 62%, respectively. The most important observation from these experiments was the fact that Pd/Al_2O_3 showed significant activity loss after exposure to NaCl or HCl solutions, whereas Pd/SOMS was not at all affected by the chloride treatments.

The decrease in the catalytic activity of Pd/Al_2O_3 was attributed to chloride bonding on Pd as evidenced by the presence of Pd-Cl scattering in EXAFS and the formation of chloride-containing Pd complexes as evidenced by XPS. The extent of the deactivation observed over HCl-treated Pd/Al_2O_3 was higher than that over NaCl-treated Pd/Al_2O_3. The additional loss in the catalytic activity was attributed to the leaching of Pd during the treatment with 0.01 M HCl solution.

Activity experiments were also performed in the presence of 10% ethanol in the reaction medium to observe the catalytic performance of HCl-treated catalyst when Pd/SOMS was kept swollen under reaction conditions. It was previously reported that having ethanol in the reaction medium enhances the kinetics of HDC of TCE over Pd/SOMS due to swelling and increases the tunable accessibility of the active sites induced by organic swelling agents [34]. Fig. 6 shows TCE conversion with respect to time observed in the absence and presence of 10% ethanol in the reaction medium over pristine and HCl-treated Pd/SOMS. Presence of 10% ethanol in the reaction medium increased the TCE conversion observed over pristine Pd/SOMS from 62% to 99% at the end of six hours. With the experiments performed in the presence of 10% ethanol in the reaction medium, the catalytic activity of pristine Pd/SOMS was shown to be similar to that of HCl-treated Pd/SOMS. These results further confirm that Pd/SOMS was not affected from the chloride treatments.

3.7. Additional remarks about the deactivation resistance of Pd/SOMS

Deactivation due to chloride species is one of the problems of HDC catalysts which impede the commercialization and widespread utilization of HDC as a remediation technique. As mentioned in the Introduction, chloride exposure does not only cause metal-chloride formations, but also favors other deactivation modes, including

leaching, carbon deposition, and metal sintering [1,6,13–19]. The aqueous phase chloride treatments employed in this study were performed under an inert atmosphere and at room temperature. Therefore, carbon deposition and metal sintering are unlikely to be the modes of deactivation since the chloride treatment does not involve any carbon-containing reagents or any high-temperature exposure. Therefore, the scope of this study was limited to investigating Pd-Cl interactions and leaching of the active metal stemmed from chloride treatments.

Post-treatment characterization experiments were performed after the treated catalyst was filtered and dried. This may raise the question whether the Pd-Cl species observed over these dried samples would bare any resemblance to the species when the catalyst is inside the liquid phase where there may be equilibrium established between the surface species and aqueous species. To examine the strength of these complexes, a temperature programmed reaction experiment with hydrogen was performed over Pd/Al_2O_3 treated by 0.1 M HCl. The temperature-programmed-reaction profile, given in Fig. S1, showed that HCl evolution started around 350 °C and continued until 900 °C, indicating that Pd-Cl species are stable.

In addition, laser Raman spectra were acquired over (i) Pd/Al_2O_3 after it went through the HCl-treatment and was dried, and (ii) during the HCl treatment, i.e., while Pd/Al_2O_3 was in contact with the HCl solution. The purpose of this experiment was to examine the differences between the surface species when the surface was in contact with the aqueous HCl solution and those in the dried-state. The spectrum collected over the catalyst in contact with the HCl solution, shown in Fig. S2, exhibited Pd-Cl vibrations similar to those obtained over HCl treated and dried Pd/Al_2O_3 [75,76]. The results show that there are no changes in the nature of Pd-Cl vibrations, as the Raman shifts are the same, suggesting that surface chemistry during the treatment and after the treatment are of similar nature.

The results presented so far demonstrated that Pd/SOMS is more resistant to deactivation by chloride anions in comparison to commonly-used HDC catalyst Pd/Al_2O_3. A true comparison of two catalysts is, however, an extremely difficult task since any characteristics of the catalysts may affect the catalytic performance. Having said this, we compared the initial states of the pristine catalysts, Pd/Al_2O_3 and Pd/SOMS to assess how they would affect their deactivation characteristics.

- In our previous study, the average particle size of Pd NPs was obtained by STEM as 3.1 nm and 8.2 nm for Pd/Al_2O_3 and Pd/SOMS, respectively [36]. The deactivation-resistance of Pd/SOMS cannot be related to the presence of large Pd NPs since chloride binding and chloride-induced metal leaching on Pd surfaces are more favorable over large Pd NPs due to higher coordination of Pd that increases the strength of Pd-Cl interactions [1,24,77].
- Pd NPs on pristine Pd/Al_2O_3 were partially oxidized. Nevertheless, oxidized Pd particles are expected to be more resistant to chloride deactivation because of their electron-deficient nature [14].
- The pore size distribution of water-soaked Pd/Al_2O_3 centered around 6.5 nm whereas that of water-soaked Pd/SOMS centered around 5.4 nm. Although the extent of poisoning over large pores is expected to be higher, the difference in the pore diameters of water-soaked samples is not significant enough to cause such drastic differences in the resistance to deactivation.

Therefore, the deactivation-resistance characteristic observed over Pd/SOMS is attributed to the unique properties of SOMS scaffold such as extreme its hydrophobicity and its swellable nature rather than the differences in the initial state of the pristine Pd/Al_2O_3 and Pd/SOMS.

4. Conclusions

The deactivation-resistance characteristics of Pd/Al_2O_3 and Pd/SOMS toward chloride anions was investigated by aqueous-phase chloride treatments with high concentrations of NaCl and HCl. The aqueous-nature of the treatments reduced the surface area, pore volume, and pore size of Pd/Al_2O_3 due to surface hydration. It should be noted that treatments in aqueous media are expected to render the initial characteristics of this catalyst more relevant to the reaction conditions. In addition, treating Pd/Al_2O_3 with chloride-containing solutions caused the adsorption of chloride species on the surface and formation of Pd-Cl complexes. When the chloride treatment was performed with HCl, significant amount of Pd was lost due to leaching. Pd/SOMS, however, exhibited strong resistance to chloride poisoning and active metal leaching. The textural properties of Pd/SOMS remained unchanged since the hydrophobic nature of Pd/SOMS minimized the interactions of water with the surface of Pd/SOMS. Catalytic activity experiments performed over pristine and treated samples of Pd/Al_2O_3 and Pd/SOMS reflected the differences in the deactivation behavior of these two catalysts. Catalytic activity decreases were noted when treated Pd/Al_2O_3 samples were tested for HDC of TCE. The catalytic activity of Pd/SOMS, however, remained unaffected by the chloride treatments.

With the investigations presented in this paper, we demonstrated the deactivation-resistant nature of Pd/SOMS to chloride-containing solutions, in comparison to a commonly-used HDC catalyst, Pd/Al_2O_3. The resistance to chloride poisoning and Pd leaching achieved over Pd/SOMS originate from the unique characteristics of SOMS scaffold, such as hydrophobicity and tunable accessibility of Pd sites through a stimuli-induced swelling behavior where the stimuli is the concentration of organic swelling agents that SOMS is exposed to.

Acknowledgements

The financial support for this work wasprovided by the National Science Foundation through the Grant CBET-1436729 and Ohio Coal Research Consortium. The authors wish to thank Dr. Lisa Hommel for her assistances in XPS data acquisition. JTM was supported as part of the National Science Foundation Energy Research Center for Innovative and Strategic Transformation of Alkane Resources (CISTAR) under the Cooperative Agreement No. EEC-1647722.

This study made use of the Materials Research Collaborative Access Team's (MRCAT) sector 10-ID-B. MRCAT operations are supported by the Department of Energy and the MRCAT member institutions. This research used resources of the Advanced Photon Source, a U.S. Department of Energy (DOE) Office of Science User Facility operated for the DOE Office of Science by Argonne National Laboratory under Contract No. DE-AC02-06CH11357. This study also made use of the Trace Element Research Laboratory (TERL) at OSU for ICP-OES experiments.

Appendix A. Supplementary data

Supplementary material related to this article can be found, in the online version, at doi:https://doi.org/10.1016/j.apcatb.2018.08.065.

References

[1] G. Yuan, M.A. Keane, Liquid phase hydrodechlorination of chlorophenols over Pd/C and Pd/Al2O3: a consideration of HCl/catalyst interactions and solution pH effects, Appl. Catal. B 52 (2004) 301–314.
[2] B. Coq, G. Ferrat, F. Figueras, Conversion of chlorobenzene over palladium and rhodium catalysts of widely varying dispersion, J. Catal. 101 (1986) 434–445.
[3] J.W. Bozzelli, Y.-M. Chen, S.S.C. Chuang, Catalytic hydrodechlorination of 1,2-dichloroethane and trichloroethylene over Rh/Si02 catalysts, Chem. Eng. Commun. 115 (1992) 1–11.
[4] S. Ordóñez, H. Sastre, F. Díez, Hydrodechlorination of organochlorinated aliphatic compounds over nickel catalysts, React. Kinet. Catal. Lett. 70 (2000) 61–66.
[5] S. Ordóñez, H. Sastre, F.V. Díez, Hydrodechlorination of tetrachloroethylene over modified red mud: deactivation studies and kinetics, Appl. Catal. B 34 (2001) 213–226.
[6] S. Ordóñez, H. Sastre, F.V. Díez, Thermogravimetric determination of coke deposits on alumina-supported noble metal catalysts used as hydrodechlorination catalysts, Thermochim. Acta 379 (2001) 25–34.

[7] S. Ordóñez, F.V. Díez, H. Sastre, Characterisation of the deactivation of platinum and palladium supported on activated carbon used as hydrodechlorination catalysts, Appl. Catal. B 31 (2001) 113–122.
[8] D. Fritsch, K. Kuhr, K. Mackenzie, F.-D. Kopinke, Hydrodechlorination of chloroorganic compounds in ground water by palladium catalysts: part 1. Development of polymer-based catalysts and membrane reactor tests, Catal. Today 82 (2003) 105–118.
[9] C. Namasivayam, D. Kavitha, Adsorptive removal of 2-chlorophenol by low-cost coir pith carbon, J. Hazard. Mater. 98 (2003) 257–274.
[10] W.W. McNab, R. Ruiz, M. Reinhard, In-situ destruction of chlorinated hydrocarbons in groundwater using catalytic reductive dehalogenation in a reactive well: testing and operational experiences, Environ. Sci. Technol. 34 (2000) 149–153.
[11] G.V. Lowry, M. Reinhard, Pd-catalyzed TCE dechlorination in groundwater: solute effects, biological control, and oxidative catalyst regeneration, Environ. Sci. Technol. 34 (2000) 3217–3223.
[12] K.N. Heck, M.O. Nutt, P. Alvarez, M.S. Wong, Deactivation resistance of Pd/Au nanoparticle catalysts for water-phase hydrodechlorination, J. Catal. 267 (2009) 97–104.
[13] A. Gampine, D.P. Eyman, Catalytic hydrodechlorination of chlorocarbons. 2. Ternary oxide supports for catalytic conversions of 1,2-dichlorobenzene, J. Catal. 179 (1998) 315–325.
[14] R. Gopinath, N. Lingaiah, B. Sreedhar, I. Suryanarayana, P.S. Sai Prasad, A. Obuchi, Highly stable Pd/CeO2 catalyst for hydrodechlorination of chlorobenzene, Appl. Catal. B 46 (2003) 587–594.
[15] B. Coq, Conversion under hydrogen of dichlorodifluoromethane over supported palladium catalysts, J. Catal. 141 (1993) 21–33.
[16] B. Coq, Conversion of chlorobenzene over palladium and rhodium catalysts of widely varying dispersion, J. Catal. 101 (1986) 434–445.
[17] G. Yuan, M.A. Keane, Role of base addition in the liquid-phase hydrodechlorination of 2,4-dichlorophenol over Pd/Al2O3 and Pd/C, J. Catal. 225 (2004) 510–522.
[18] E. Lopez, S. Ordonez, F. Diez, Deactivation of a Pd/Al2O3 catalyst used in hydrodechlorination reactions: influence of the nature of organochlorinated compound and hydrogen chloride, Appl. Catal. B 62 (2006) 57–65.
[19] D.Ju Moon, M. Jo Chung, K. You Park, S.In Hong, Deactivation of Pd catalysts in the hydrodechlorination of chloropentafluoroethane, Appl. Catal. A Gen. 168 (1998) 159–170.
[20] Y. Ukisu, T. Miyadera, Hydrogen-transfer hydrodehalogenation of aromatic halides with alcohols in the presence of noble metal catalysts, J. Mol. Catal. a-Chem. 125 (1997) 135–142.
[21] M.I. Cobo, J.A. Conesa, C.M. de Correa, The effect of NaOH on the liquid-phase hydrodechlorination of dioxins over Pd/gamma-Al2O3, J. Phys. Chem. A 112 (2008) 8715–8722.
[22] Y. Ukisu, T. Miyadera, Dechlorination of dioxins with supported palladium catalysts in 2-propanol solution, Appl. Catal. A Gen. 271 (2004) 165–170.
[23] V. Felis, C. De Bellefon, P. Fouilloux, D. Schweich, Hydrodechlorination and hydrodearomatisation of monoaromatic chlorophenols into cyclohexanol on Ru/C catalysts applied to water depollution: influence of the basic solvent and kinetics of the reactions, Appl. Catal. B 20 (1999) 91–100.
[24] T. Janiak, J. Okal, Effectiveness and stability of commercial Pd/C catalysts in the hydrodechlorination of meta-substituted chlorobenzenes, Appl. Catal. B 92 (2009) 384–392.
[25] M.A. Keane, Supported transition metal catalysts for hydrodechlorination reactions, ChemCatChem 3 (2011) 800–821.
[26] S. Ordonez, B.P. Vivas, F.V. Diez, Minimization of the deactivation of palladium catalysts in the hydrodechlorination of trichloroethylene in wastewaters, Appl. Catal. B 95 (2010) 288–296.
[27] B.P. Chaplin, M. Reinhard, W.F. Schneider, C. Schuth, J.R. Shapley, T.J. Strathmann, C.J. Werth, Critical review of Pd-based catalytic treatment of priority contaminants in water, Environ. Sci. Technol. 46 (2012) 3655–3670.
[28] M.O. Nutt, J.B. Hughes, M.S. Wong, Designing Pd-on-Au bimetallic nanoparticle catalysts for trichloroethene hydrodechlorination, Environ. Sci. Technol. 39 (2005) 1346–1353.
[29] M.O. Nutt, K.N. Heck, P. Alvarez, M.S. Wong, Improved Pd-on-Au bimetallic nanoparticle catalysts for aqueous-phase trichloroethene hydrodechlorination, Appl. Catal. B 69 (2006) 115–125.
[30] C. Schüth, S. Disser, F. Schüth, M. Reinhard, Tailoring catalysts for hydrodechlorinating chlorinated hydrocarbon contaminants in groundwater, Appl. Catal. B 28 (2000) 147–152.
[31] C. Schüth, N.-A. Kummer, C. Weidenthaler, H. Schad, Field application of a tailored catalyst for hydrodechlorinating chlorinated hydrocarbon contaminants in groundwater, Appl. Catal. B 52 (2004) 197–203.
[32] F.-D. Kopinke, D. Angeles-Wedler, D. Fritsch, K. Mackenzie, Pd-catalyzed hydrodechlorination of chlorinated aromatics in contaminated waters—effects of surfactants, organic matter and catalyst protection by silicone coating, Appl. Catal. B 96 (2010) 323–328.
[33] R. Navon, S. Eldad, K. Mackenzie, F.-D. Kopinke, Protection of palladium catalysts for hydrodechlorination of chlorinated organic compounds in wastewaters, Appl. Catal. B 119–120 (2012) 241–247.
[34] G. Celik, S.A. Ailawar, H. Sohn, Y. Tang, F.F. Tao, J.T. Miller, P.L. Edmiston, U.S. Ozkan, Swellable organically modified silica (SOMS) as a catalyst scaffold for catalytic treatment of water contaminated with trichloroethylene, ACS Catal. (2018) 6796–6809.
[35] G. Celik, S.A. Ailawar, S. Gunduz, P.L. Edmiston, U.S. Ozkan, Formation of carbonaceous deposits on Pd-based hydrodechlorination catalysts: vibrational spectroscopy investigations over Pd/Al2O3 and Pd/SOMS, Catal. Today (2018), https://doi.org/10.1016/j.cattod.2018.05.001.
[36] H. Sohn, G. Celik, S. Gunduz, S.L. Dean, E. Painting, P.L. Edmiston, U.S. Ozkan, Hydrodechlorination of trichloroethylene over Pd supported on swellable organically-modified silica (SOMS), Appl. Catal. B 203 (2017) 641–653.
[37] H. Sohn, G. Celik, S. Gunduz, S.S. Majumdar, S.L. Dean, P.L. Edmiston, U.S. Ozkan, Effect of high-temperature on the swellable organically-modified silica (SOMS) and its application to gas-phase hydrodechlorination of trichloroethylene, Appl. Catal. B 209 (2017) 80–90.
[38] C.M. Burkett, P.L. Edmiston, Highly swellable sol–gels prepared by chemical modification of silanol groups prior to drying, J. Non-Cryst. Solids 351 (2005) 3174–3178.
[39] C.M. Burkett, L.A. Underwood, R.S. Volzer, J.A. Baughman, P.L. Edmiston, Organic–inorganic hybrid materials that rapidly swell in non-polar liquids: nanoscale morphology and swelling mechanism, Chem. Mater. 20 (2008) 1312–1321.
[40] P.L. Edmiston, L.A. Underwood, Absorption of dissolved organic species from water using organically modified silica that swells, Sep. Purif. Technol. 66 (2009) 532–540.
[41] P.L. Edmiston, L.J. West, A. Chin, N. Mellor, D. Barth, Adsorption of gas phase organic compounds by swellable organically modified silica, Ind. Eng. Chem. Res. 55 (2016) 12068–12079.
[42] P.L. Edmiston, C. Osborne, K.P. Reinbold, D.C. Pickett, L.A. Underwood, Pilot scale testing composite swellable organosilica nanoscale zero-valent iron-Iron-Osorb®-for in situ remediation of trichloroethylene, Remediat. J. 22 (2011) 105–123.
[43] C.U. Segre, N.E. Leyarovska, L.D. Chapman, W.M. Lavender, P.W. Plag, A.S. King, A.J. Kropf, B.A. Bunker, K.M. Kemner, P. Dutta, R.S. Duran, J. Kaduk, The MRCAT insertion device beamline at the advanced photon source, AIP Conf. Proc. 521 (2000) 419–422.
[44] T. Ressler, WinXAS: a new software package not only for the analysis of energy-dispersive XAS data, J. Phys. Iv 7 (1997) 269–270.
[45] G. Celik, Swellable Organically Modified Silica As a Novel Catalyst Scaffold for Catalytic Treatment of Water Contaminated With Trichloroethylene, William G. Lowrie Chemical and Biomolecular Engineering, The Ohio State University, Columbus, Ohio, USA, 2018.
[46] O. Levenspiel, Chemical Reaction Engineering, 3rd ed., John Wiley & Sons, 1999.
[47] K.S.W. Sing, Reporting physisorption data for gas/solid systems with special reference to the determination of surface area and porosity (Recommendations 1984), Pure Appl. Chem. 57 (1985) 603–619.
[48] M.P. Tsyurupa, V.A. Davankov, Porous structure of hypercrosslinked polystyrene: state-of-the-art mini-review, React. Funct. Polym. 66 (2006) 768–779.
[49] J.C. Groen, L.A.A. Peffer, J. Pérez-Ramírez, Pore size determination in modified micro- and mesoporous materials. Pitfalls and limitations in gas adsorption data analysis, Microporous Mesoporous Mater. 60 (2003) 1–17.
[50] J.B. Peri, R.B. Hannan, Surface hydroxyl groups on γ-Alumina1, J. Phys. Chem. 64 (1960) 1526–1530.
[51] A.V. Deo, I.G. Dalla Lana, Infrared study of the adsorption and mechanism of surface reactions of 1-propanol on. gamma.-alumina and. gamma.-alumina doped with sodium hydroxide and chromium oxide, J. Phys. Chem. 73 (1969) 716–723.
[52] J.M. van Middlesworth, S.A. Wood, The stability of palladium(II) hydroxide and hydroxy-chloride complexes: an experimental solubility study at 25-85 degrees C and 1 bar, Geochim. Cosmochim. Acta 63 (1999) 1751–1765.
[53] G. Kumar, J.R. Blackburn, R.G. Albridge, W.E. Moddeman, M.M. Jones, Photoelectron spectroscopy of coordination compounds. II. Palladium complexes, Inorg. Chem. 11 (1972) 296–300.
[54] R.F. Bueres, E. Asedegbega-Nieto, E. Diaz, S. Ordonez, F.V. Diez, Performance of carbon nanofibres, high surface area graphites, and activated carbons as supports of Pd-based hydrodechlorination catalysts, Catal. Today 150 (2010) 16–21.
[55] R.F. Bueres, E. Asedegbega-Nieto, E. Diaz, S. Ordonez, F.V. Diez, Preparation of carbon nanofibres supported palladium catalysts for hydrodechlorination reactions, Catal. Commun. 9 (2008) 2080–2084.
[56] J.F. Moulder, J. Chastain, Handbook of X-ray Photoelectron Spectroscopy: A Reference Book of Standard Spectra for Identification and Interpretation of XPS Data, Physical Electronics Division, Perkin-Elmer Corporation, 1992.
[57] Y. Zhao, W. Liang, Y. Li, L. Lefferts, Effect of chlorine on performance of Pd catalysts prepared via colloidal immobilization, Catal. Today 297 (2017) 308–315.
[58] A. Shchukarev, J.-F. Boily, A.R. Felmy, XPS of fast-frozen hematite colloids in NaCl aqueous solutions: I. Evidence for the formation of multiple layers of hydrated sodium and chloride ions induced by the {001} basal plane, J. Phys. Chem. C 111 (2007) 18307–18316.
[59] L. Bodenes, A. Darwiche, L. Monconduit, H. Martinez, The Solid Electrolyte Interphase a key parameter of the high performance of Sb in sodium-ion batteries: comparative X-ray Photoelectron Spectroscopy study of Sb/Na-ion and Sb/Li-ion batteries, J. Power Sources 273 (2015) 14–24.
[60] B. Pawelec, A.M. Venezia, V. La Parola, E. Cano-Serrano, J.M. Campos-Martin, J.L.G. Fierro, AuPd alloy formation in Au-Pd/Al2O3 catalysts and its role on aromatics hydrogenation, Appl. Surf. Sci. 242 (2005) 380–391.
[61] J.T. Miller, A.J. Kropf, Y. Zha, J.R. Regalbuto, L. Delannoy, C. Louis, E. Bus, J.A. van Bokhoven, The effect of gold particle size on Au-Au bond length and reactivity toward oxygen in supported catalysts, J. Catal. 240 (2006) 222–234.
[62] M.W. Tew, J.T. Miller, J.A. van Bokhoven, Particle size effect of hydride formation and surface hydrogen adsorption of nanosized palladium catalysts: L-3 edge vs K edge X-ray absorption spectroscopy, J. Phys. Chem. C 113 (2009) 15140–15147.
[63] J.A. McCaulley, In-situ x-ray absorption spectroscopy studies of hydride and carbide formation in supported palladium catalysts, J. Phys. Chem. 97 (1993) 10372–10379.
[64] D. Tessier, A. Rakai, F. Bozonverduraz, Spectroscopic study of the interaction of carbon monoxide with cationic and metallic palladium in palladium–alumina catalysts, J. Chem. Soc.-Faraday Trans. 88 (1992) 741–749.

[65] R.S. Monteiro, L.C. Dieguez, M. Schmal, The role of Pd precursors in the oxidation of carbon monoxide over Pd/Al2O3 and Pd/CeO2/Al2O3 catalysts, Catal. Today 65 (2001) 77–89.
[66] R. Craciun, W. Daniell, H. Knozinger, The effect of CeO2 structure on the activity of supported Pd catalysts used for methane steam reforming, Appl. Catal. A Gen. 230 (2002) 153–168.
[67] R.M. Navarro, B. Pawelec, J.M. Trejo, R. Mariscal, J.L.G. Fierro, Hydrogenation of aromatics on sulfur-resistant PtPd bimetallic catalysts, J. Catal. 189 (2000) 184–194.
[68] D. Amalric-Popescu, F. Bozon-Verduraz, Infrared studies on SnO2 and Pd/SnO2, Catal. Today 70 (2001) 139–154.
[69] E.A. Sales, J. Jove, M.D. Mendes, F. Bozon-Verduraz, Palladium, palladium-tin, and palladium-silver catalysts in the selective hydrogenation of hexadienes: TPR, Mossbauer, and infrared studies of adsorbed CO, J. Catal. 195 (2000) 88–95.
[70] G. Agostini, R. Pellegrini, G. Leofanti, L. Bertinetti, S. Bertarione, E. Groppo, A. Zecchina, C. Lamberti, Determination of the particle size, available surface area, and nature of exposed sites for silica-alumina-supported Pd nanoparticles: a multitechnical approach, J. Phys. Chem. C 113 (2009) 10485–10492.
[71] L.M. Esteves, M.H. Brijaldo, F.B. Passos, Decomposition of acetic acid for hydrogen production over Pd/Al2O3 and Pd/TiO2: influence of metal precursor, J. Mol. Catal. A Chem. 422 (2016) 275–288.
[72] B. Pawelec, R. Mariscal, R.M. Navarro, S. van Bokhorst, S. Rojas, J.L.G. Fierro, Hydrogenation of aromatics over supported Pt-Pd catalysts, Appl. Catal. A Gen. 225 (2002) 223–237.
[73] A.M. Venezia, V. La Parola, G. Deganello, B. Pawelec, J.L.G. Fierro, Synergetic effect of gold in Au/Pd catalysts during hydrodesulfurization reactions of model compounds, J. Catal. 215 (2003) 317–325.
[74] S. Bertarione, C. Prestipino, E. Groppo, D. Scarano, G. Spoto, A. Zecchina, R. Pellegrini, G. Leofanti, C. Lamberti, Direct IR observation of vibrational properties of carbonyl species formed on Pd nano-particles supported on amorphous carbon: comparison with Pd/SiO2-Al2O3, Phys. Chem. Chem. Phys. 8 (2006) 3676–3681.
[75] C. Drew Tait, D.R. Janecky, P.S.Z. Rogers, Speciation of aqueous palladium(II) chloride solutions using optical spectroscopies, Geochim. Cosmochim. Acta 55 (1991) 1253–1264.
[76] S.F. Parker, H. Herman, A. Zimmerman, K.P.J. Williams, The vibrational spectrum of K2PdCl4: first detection of the silent mode ν5, Chem. Phys. 261 (2000) 261–266.
[77] J.L. Benitez, G. Del Angel, Effect of chlorine released during hydrodechlorination of chlorobenzene over Pd, Pt and Rh supported catalysts, React. Kinet. Catal. Lett. 70 (2000) 67–72.